

Spectroscopic ellipsometry study of $\text{Zn}_{1-x}\text{Co}_x\text{Se}$ alloys grown on GaAs

Y. D. Kim

*Department of Physics and Materials Research Laboratory, University of Illinois at Urbana-Champaign, Illinois 61801
and Department of Physics, Kyung Hee University, Seoul 130-701, Korea*

S. L. Cooper and M. V. Klein

Department of Physics and Materials Research Laboratory, University of Illinois at Urbana-Champaign, Illinois 61801

J.-H. Park

AT&T Bell Laboratories, Murray Hill, New Jersey 07974

B. T. Jonker

Naval Research Laboratory, Washington, DC 20375-5000

(Received 5 May 1994)

We present an ellipsometric study of $\text{Zn}_{1-x}\text{Co}_x\text{Se}$ films with $0 \leq x < 0.1$ grown on GaAs substrates. We attribute the significant distortions of the interference patterns at energies between 1.6 and 1.8 eV to absorption due to localized d -state transitions between the crystal-field levels of Co^{2+} ions on Zn sites. There is also evidence of an absorption feature near 4.3 eV within the $E_0 + \Delta_0 - E_1$ band-gap region. We propose that this structure has the characteristics of a charge-transfer-type p -to- d transition. A similar absorption band also seems to be present in $\text{Zn}_{1-x}\text{Fe}_x\text{Se}$ system.

I. INTRODUCTION

Diluted magnetic semiconductors (DMS's) (Refs. 1 and 2) are a class of semiconducting materials formed by randomly replacing some of the cations in a compound semiconductor with magnetic ions. The electronic structure of the host II-VI compounds, in which the valence (conduction) bands are characterized by cation- s -anion- p bonding (antibonding) states, are explained well by one-electron band theory.³ However, the transition-metal ions introduced into the host commonly contain a partially filled $3d$ shell, and it is uncertain that the one-electron picture is still appropriate for fully describing the electronic structure of DMS's. A number of optical-absorption spectra have been measured for various DMS systems,⁴ and all measured spectra exhibit excited multiplet states which correspond to intra- d shell transitions. These observed multiplets are not consistent with simple one-electron theory. The one-electron model combined with many-electron multiplet effects has been adopted to explain the optical spectra observed by many groups.^{5,6}

Recently, we studied the $\text{Zn}_{1-x}(\text{Mn},\text{Fe},\text{Co})_x\text{Se}$ system in the energy range 3.5–5.5 eV using spectroscopic ellipsometry (SE).^{7,8} In our study, the composition-dependent E_1 and $E_1 + \Delta_1$ band-gap energies were well explained by the hybridization interaction between ZnSe sp bands and magnetic impurity d states. But a structure which appears at around 4.3 eV in the $\text{Zn}_{1-x}\text{Co}_x\text{Se}$ spectra was not accounted for. In the present work, which covers a wider spectral range, we apply a many-body approach involving the Anderson impurity Hamiltonian^{9–11} to explain the origin of this 4.3-eV transition. This model, which extends the Mott-Hubbard picture^{12–15} to include the transfer of an electron from the itinerant ligand (sp) band to localized transition metal $3d$ states, has been successfully applied to explain the electronic structure of transition-metal compounds,^{9,16–18} and should be suit-

able to explain transitions associated with strongly correlated CO (Fe,Mn) $3d$ electrons.

Distortions in the interference patterns were also observed in $\text{Zn}_{1-x}\text{Co}_x\text{Se}$ at 1.6–1.8 eV, and interpreted as internal d - d transitions of Co^{2+} in the tetrahedral crystal field of ZnSe. The first observation of the $E_0 + \Delta_0$ band-gap energies at a small composition range in $\text{Zn}_{1-x}\text{Co}_x\text{Se}$ are also reported.

II. EXPERIMENTAL DETAILS

Pseudodielectric function spectra $\langle \epsilon(\omega) \rangle = \langle \epsilon_1(\omega) \rangle + i \langle \epsilon_2(\omega) \rangle$ of $\text{Zn}_{1-x}\text{Co}_x\text{Se}$ layers grown by molecular-beam epitaxy (MBE) on GaAs(001) substrates were measured at room temperature between 1.5 and 6.0 eV using an automatic spectroscopic rotating analyzer ellipsometer of the type developed by Aspnes.^{19,20} Since the thickness of the layers ranged from 0.28 to 2 μm , which is substantially larger than the critical thickness for strain relaxation,^{21–23} the measurements are expected to reflect the dielectric response of bulk $\text{Zn}_{1-x}\text{Co}_x\text{Se}$. Experimental details and growth conditions were reported in previous works.^{7,24}

It is well known that the existence of overlayers on the surface complicates efforts to obtain the intrinsic dielectric response of a material by ellipsometry because of the surface sensitivity of this technique.²⁵ Therefore, we followed the wet chemical etching procedure described in Ref. 24. The chemical treatment [1:3 mixture of NH_4OH (29%): methanol] was repeated until real-time ellipsometric spectra showed no more changes, and the highest values of ϵ_2 at the $E_1 + \Delta_1$ (or the highest values of ϵ_1 at E_1) band-gap energy region were obtained. Figure 1 shows the real (ϵ_1) and imaginary (ϵ_2) parts of the pseudodielectric function after the chemical treatment of one of the samples ($\text{Zn}_{0.984}\text{Co}_{0.016}\text{Se}$). The significant enhancement of both real and imaginary parts of the

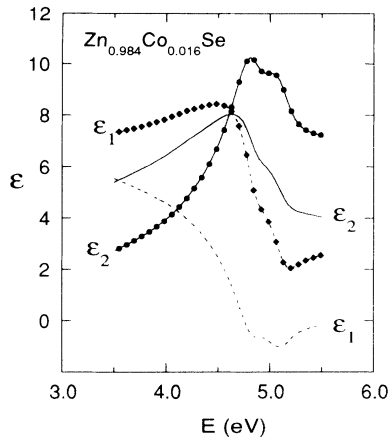


FIG. 1. Pseudodielectric function of $\text{Zn}_{0.984}\text{Co}_{0.016}\text{Se}$ film before (lines) and after (lines with filled symbols) the chemical etching method described in Ref. 24. The enhancement of the structures is easily seen.

spectrum is easily seen, demonstrating that overlayers identified as natural surface oxide layers²⁴ were successfully removed.

To obtain the interband transition energies, the second derivatives of the dielectric spectra were numerically calculated.²⁶ An appropriate level of smoothing was also allowed in order to suppress the noise in the derivative spectra without distorting the line shape. The resulting spectra were fitted to the standard analytic critical point (CP) (interband transition) line shape.^{27,28}

$$\frac{d^2\epsilon}{d\omega^2} = \begin{cases} n(n-1)Ae^{i\phi}(\omega-E+i\Gamma)^{n-2}, & n \neq 0 \\ Ae^{i\phi}(\omega-E+i\Gamma)^{-2}, & n = 0, \end{cases} \quad (1)$$

where a critical point is described by the amplitude A , threshold energy E , broadening Γ , and excitonic phase angle ϕ . The exponent $n = -1$ is chosen as an excitonic CP line shape as previously reported.^{7,24,29,30} A least-squares procedure was used for the fit, with both the real and the imaginary parts of $d^2\epsilon/d\omega^2$ fitted simultaneously.

III. RESULTS AND DISCUSSIONS

A. Intra- d shell transitions

Due to the atomlike character of the $3d$ transition-metal impurity electrons [$\text{Co}^{2+}(3d^7)$], the intra- d shell transitions associated with the crystal-field split states have been observed in the optical absorption spectra by different groups. In the $\text{Zn}_{1-x}\text{Co}_x\text{Se}$ spectra for $x \geq 0.04$, we observe distortions in the interference patterns between 1.6–1.8 eV. Figure 2 shows that the clean and periodic interference pattern of pure ZnSe in the transparent region below the fundamental band gap becomes obviously distorted by some subband gap absorption as the Co composition increases. Since this 1.6–1.8-eV energy is in the same energy range as that calculated

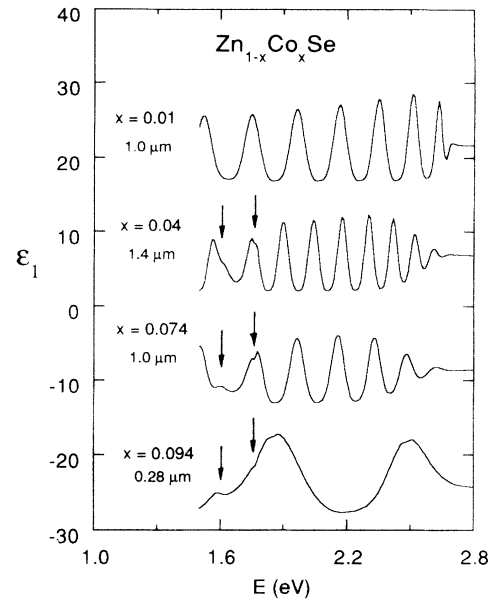


FIG. 2. Real parts of pseudodielectric function, $\langle \epsilon \rangle$, of $\text{Zn}_{1-x}\text{Co}_x\text{Se}$ in the transparent range of 1.5–2.4 eV. Spectra have been offset by 15 from each other from the center spectrum of the $x = 0.04$ sample.

and experimentally observed^{5,31–34} for ${}^4A_2(F) \rightarrow {}^4T_1(P)$ transition of Co^{2+} in ZnSe under a tetrahedral crystal field, we attribute this distortion to the intra- d shell transitions of Co^{2+} in ZnSe. To our knowledge, this is the first ellipsometric observation of such absorptions below the fundamental band-gap energy. Extracting the dielectric response of the $\text{Zn}_{1-x}\text{Co}_x\text{Se}$ film using a multilayer calculation (air/ $\text{Zn}_{1-x}\text{Co}_x\text{Se}$ /GaAs) (Ref. 35) can directly reveal the underlying physics. However, because of the presence of an interface layer between the film and the GaAs substrate,²⁴ and the uncertainty of the film thickness, we show a model calculation in Fig. 3 instead. The simplest way to approximately model the dielectric function for a film is to use a harmonic-oscillator model.³⁶ We chose two oscillators with transition energies 1.67 and 1.83 eV, amplitudes 0.012 and 0.01, and linewidths of 0.04 eV. The GaAs substrate dielectric function was approximated as $\epsilon = 14.6 + i1.4$, which is the averaged dielectric function for GaAs in this energy range. Figure 3(a) shows the calculated dielectric function of the film, and Fig. 3(b) is the result of the pseudodielectric function we obtained with a three-phase model calculation using a film thickness of 1.4 μm . Despite the simplified model calculation, the resulting pseudodielectric function shows nearly the same behavior as our measured pseudodielectric response shown in Fig. 2 (1.4 μm , $x = 0.04$). The resulting absorption bands at 1.67 and 1.83 eV in Fig. 3(a) are consistent with the reported absorption experimental data below the fundamental band gap of ZnSe:Co in Refs. 5 and 31–34. Therefore, we conclude that this result shows clear existence of the absorptions due to intra- d to d transitions of Co ions under a tetrahedral crystal field.

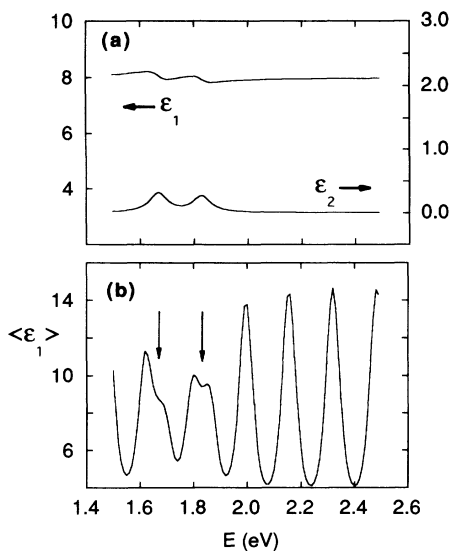


FIG. 3. Three-layer (air/film/substrate) model calculation. (a) The film dielectric function is modeled by two harmonic oscillators with a constant background $7.0+i0.0$, which is the averaged dielectric function for ZnSe in this energy range. (b) The calculated pseudodielectric function shows behavior similar to our measured spectrum of the $1.4\text{-}\mu\text{m}$, $x=0.04$ sample.

B. $E_0 + \Delta_0$ peaks

To our knowledge, no data are available concerning the $E_0 + \Delta_0$ band gaps of $\text{Zn}_{1-x}\text{Co}_x\text{Se}$ alloys. Because the film thicknesses were large enough in our samples to confine interference patterns below 3.0 eV , we have been able to measure the $E_0 + \Delta_0$ peak near 3.11 eV by spectroscopic ellipsometry at room temperature up to $x=0.04$. The second derivative spectra and their fits to Eq. (1) are shown in Fig. 4. We find that the room-temperature $E_0 + \Delta_0$ band gap increases with x with an approximate slope of $0.5\text{ eV}/x$. Note that a slight initial decrease or “bowing” is observed at $x=0.076$, which is not yet understood and more systematic study is needed. Accounting for the difference in measurement temperature, this value is comparable to the reported slope of E_0 by reflectivity measurement at 5 K in Refs. 37 and 38 (slope = $0.743\text{ eV}/x$). Our results contrast with a recent photoluminescence study³⁹ showing a decrease of the E_0 band-gap energy with increasing composition. Since both $E_0(\Gamma_8^v \rightarrow \Gamma_6^c)$ and $E_0 + \Delta_0(\Gamma_7^v \rightarrow \Gamma_6^c)$ transitions occur at the same Γ -point in the Brillouin zone,⁴⁰ from a symmetry point of view, we expect a similar composition dependence for the two transitions. More experimental studies, including transmission experiments, are necessary to clarify this discrepancy.

C. Charge-transfer-type transition

We also observed a structure near 4.3 eV in $\text{Zn}_{1-x}\text{Co}_x\text{Se}$, which appears when $x \geq 0.04$ and grows with x (Fig. 5). This structure appears along with the intra- d shell transitions of Co^{2+} in the $1.6\text{--}1.8\text{ eV}$ energy region, and so the origin of the structure appears to be as-

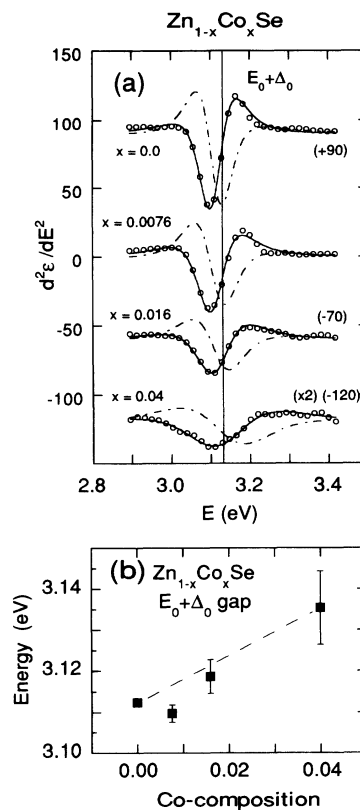


FIG. 4. (a) Fits to the second derivatives of the real (solid) and imaginary (dot-dashed) parts of the dielectric function of $\text{Zn}_{1-x}\text{Co}_x\text{Se}$ at the $E_0 + \Delta_0$ band-gap region. The dots represent experimental data for $d^2\epsilon_1/d\omega^2$. To show the quality of the fits clearly, we reduced the number of data points in the graph by one half. (b) Plot of the composition-dependent band gap. Additional data are necessary to quantify the band-gap bowing for $x < 0.02$.

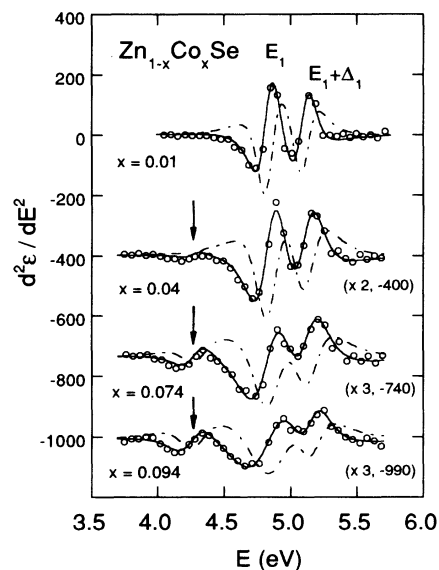


FIG. 5. Fits to the second derivatives of the real (solid lines) and imaginary (dot-dashed lines) parts of the dielectric function of $\text{Zn}_{1-x}\text{Co}_x\text{Se}$ at the E_1 and $E_1 + \Delta_1$ band-gap regions. The dots represent experimental data for $d^2\epsilon_1/d\omega^2$. To show the quality of the fits clearly, we reduced the number of data points in the graph by one fourth.

sociated with Co d -electron states. This transition, however, cannot be ascribed to an intra- d shell transition, because the maximum energy of the multiplet excitations is near 3.0 eV.⁵ Since this structure cannot be explained by the primary ZnSe sp band structure, in this section we concentrate on transitions associated with the strongly correlated d -electron system.

1. Many-body approach

In the optical-absorption spectra of insulating $3d$ transition-metal compounds, two types of transitions are often observed. One is the intra- d shell transitions which show the multiplet excitations of the $3d^n$ configuration, and the other is the anion p to transition-metal $3d$ charge-transfer transition. The latter contributes to the photoconductivities for photon energies greater than the charge-transfer energy associated with moving an electron from one site to another. We propose attributing the structure observed in $\text{Zn}_{1-x}\text{Co}_x\text{Se}$ to the Se $4p$ to Co $3d$ charge-transfer transition. Photocapacitance (photoionization) measurements³³ on this material show a clear onset around 2.2 eV (in Figs. 3 and 4 of Ref. 33) which can be understood as a charge-transfer transition. This energy is on the order of 2 eV smaller than our observed optical transition energy of 4.3 eV. This difference can be described by a many-body picture based on the Anderson impurity Hamiltonian. In this approach, the $3d$ states are modeled as local impurity states hybridized to the Se $4p$ band, and the parameters characterizing the model are the Se $4p$ to Co $3d$ charge-transfer energy Δ , the on-site $3d$ Coulomb energy U , and the hybridization T . In contrast to the one-electron states in the band picture, the states are represented by many-electron configuration states such as d^7 , $d^8\bar{L}$, $d^9\bar{L}^2$, etc., where \bar{L} denotes a Se $4p$ hole. The energy of the d^7 configuration state is lower than that of the $d^8\bar{L}$ state since the ionic ground state of Co in $\text{Zn}_{1-x}\text{Co}_x\text{Se}$ is $3d^7$ (Co^{2+}), and the energy difference is defined by the charge-transfer energy $\Delta = E(d^8\bar{L}) - E(d^7)$. Then the energy difference is $E(d^9\bar{L}^2) - E(d^8\bar{L}) = \Delta + U$. Here the Coulomb repulsion energy U between the two transferred d electrons is added to Δ . When the Se $4p$ –Co $3d$ hybridization is applied, the ground state becomes a linear combination of d^7 , $d^8\bar{L}$, $d^9\bar{L}^2$, etc. (even though the main component is the d^7 configuration), and the energy is lowered from $E(d^7)$ by the stabilization energy δ^N . Figure 6(a) shows the schematic energy diagram of an N -electron (neutral) system for $T=0$ and for $T \neq 0$.

Because the nonlocal charge-transfer transition is determined when the electron and the hole are uncorrelated, the charge-transfer energy depends not only on the ground (N -electron) state but also on the one-electron removal [$(N-1)$ -electron] states and on the one electron addition [$(N+1)$ -electron] states. The schematic energy diagrams of $(N-1)$ - and $(N+1)$ -electron systems relative to the ground-state energy are shown in Fig. 6(b). The $(N-1)$ -electron configurations are d^6 , $d^7\bar{L}$, $d^8\bar{L}^2$, etc. The energy separation between $d^7\bar{L}$ and d^6 corresponds to $U - \Delta$,^{9,17} and that between $d^7\bar{L}$ and $d^8\bar{L}^2$ is Δ . The value of Δ in the $\text{Zn}_{1-x}\text{Co}_x\text{Se}$ system is expected to

be smaller than U , since Se has small electronegativity, and so $E(d^7\bar{L}) < E(d^6)$. The $(N+1)$ -electron states are d^8 , $d^9\bar{L}$, etc., and their energy separation is $\Delta + U$. The lowest-energy states of $(N-1)$ - and $(N+1)$ -electron systems are also lowered from their $d^7\bar{L}$ and the d^8 states due to hybridization by the stabilization energies δ^{N-1} and δ^{N+1} , respectively. Since the conduction-band gap corresponds to the sum of the smallest one-electron removal ($N \rightarrow N-1$) energy E_i and the smallest one-electron addition ($N \rightarrow N+1$) energy E_a , the band gap is given by

$$E_{\text{gap}} = \Delta_{\text{th}} + 2\delta^N - \delta^{N-1} - \delta^{N+1}, \quad (2)$$

where Δ_{th} is the smallest (threshold) charge-transfer energy shown in Fig. 6(a).

2. $\text{Zn}_{1-x}\text{Co}_x\text{Se}$

An optical transition can be obtained from the Se $4p \rightarrow$ Co $2p$ transition of type $d_i^7 d_j^7 \rightarrow d_i^7 \bar{L} d_j^8$, where i and j denote different Co sites. This transition can be attributed to two processes, $d_i^7 \rightarrow d_i^7 \bar{L}$ ($N \rightarrow N-1$) and $d_j^7 \rightarrow d_j^8$ ($N \rightarrow N+1$). The transition energy becomes E_{gap} if excitonic effects are neglected. However, this interpretation can be applied to the condensed system but

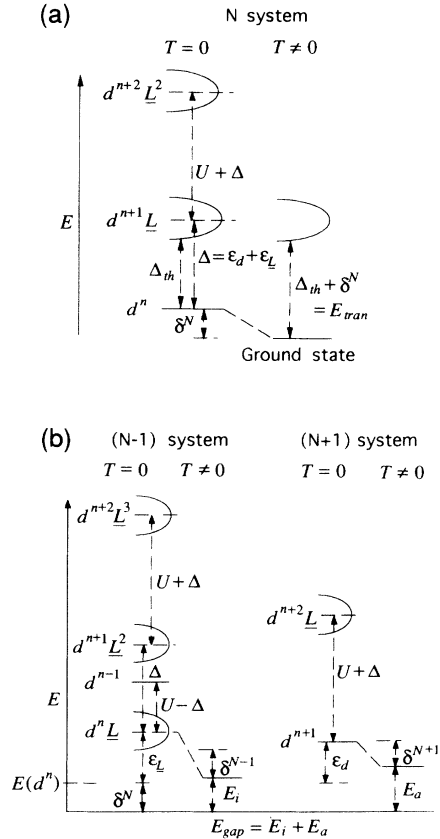


FIG. 6. (a) Energy diagram of the N -electron system from Ref. 17. The hybridization is described by T . (b) Energy diagram of $(N-1)$ - and $(N+1)$ -electron systems. Ground states are shifted by the hybridization effect T .

not to the dilute system because the distance between two different Co sites is too large for such a transition to be easily observed in the real spectrum. Hence, in the dilute limit, the charge-transfer transition reflects the transition of type $d^7 \rightarrow d^8 \underline{L}$ ($N \rightarrow N$), and the transition energy corresponds to $\Delta + \delta^N$, which is larger than E_{gap} by as much as $\delta^{N+1} + \delta^{N-1} - \delta^N$. This difference depends on Δ , U , and T , but it is observed to be the order of 2–3 eV in other systems. For example, the optical gaps of Cr_2O_3 and Fe_2O_3 are observed at ~ 3.4 eV (Ref. 41) and at ~ 1.9 eV,⁴² while those in the dilute systems of $\text{Cr}^{3+}:\text{Al}_2\text{O}_3$ and $\text{Fe}^{3+}:\text{Al}_2\text{O}_3$ are observed at ~ 5.2 eV (Ref. 43) and at > 4.7 eV,⁴⁴ respectively. Therefore, the 4.3-eV transition can be assigned to the local $d^7 \rightarrow d^8 \underline{L}$ charge-transfer transition even though the nonlocal charge-transfer transition is ~ 2.2 eV.

While our $\text{Zn}_{1-x}\text{Co}_x\text{Se}$ spectra are dominated by the local charge-transfer transition features, there is sufficient Co concentration for $x > 0.04$ to also observe features related to nonlocal charge-transfer transitions. A closer look at Fig. 2 reveals that when $x \geq 0.04$, the height of the interference pattern starts to decrease significantly above 2.2 eV. To understand this phenomenon better, we used the same multilayer model of Sec. III A. This time the dielectric function of film is modeled as in Fig. 7(a). Without any absorption below 2.7 eV (ϵ_2 is zero), the interference pattern stays at the same height until it reaches the fundamental band gap of 2.7 eV in the model. However, when we add a nonzero, increasing ϵ_2 above 2.2 eV, which approximately describes a charge-transfer transition, we can clearly observe a decrease of the interference pattern height in Fig. 7(b). Therefore we attribute this decrease to the indirect observation of a nonlocal charge transfer transition with energy at ~ 2.2 eV. This value is the same as that observed in the photocapacitance measurement.³³

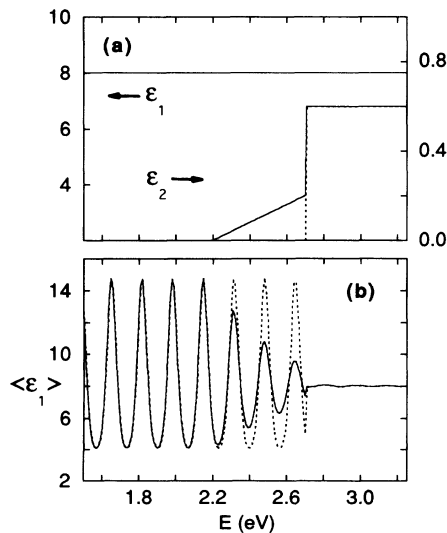


FIG. 7. (a) Model dielectric function of the film with (solid line) and without (dotted line) charge-transfer-type absorption. (b) The calculated pseudodielectric function with absorption shows behavior similar to our measured spectrum.

3. $\text{Zn}_{1-x}\text{Fe}_x\text{Se}$

We also observe similar behavior in $\text{Zn}_{1-x}\text{Fe}_x\text{Se}$ alloys at around 3.6 eV, as shown in Fig. 8. Because of the relatively small thickness, the $E_0 + \Delta_0$ structure in the $x = 0.088$ spectrum is distorted significantly, but interference patterns clearly stop below 3.2 eV. Therefore the small growing peak indicated by arrows in the future is a structure that cannot be explained by the zinc-blende sp band structure. In contrast to the Co case, the 3.6-eV structure in the $\text{Zn}_{1-x}\text{Fe}_x\text{Se}$ film is very broad, so that the second derivative does not enhance the structure significantly. We associate the weaker and broader signals in the Fe films as due to different crystal-field effects in the Fe case. The ionic ground state of Co^{2+} is d^7 (4A_2) in a tetrahedral crystal field, which has three holes in the higher t_{2g} orbital and the fully filled lower e_g orbital. Therefore, the transferred electron can only fill the t_{2g} orbital. For the case of Fe^{2+} the ionic ground state is d^6 (4E), which has one e_g hole as well as three t_{2g} holes. The charge-transfer states with the lower energy are preferable, so that the transferred electron fills the e_g hole. Therefore, the charge-transfer transition probability in the Fe case should be smaller by a factor of 3 than that in the Co case. The 1.26-eV (Ref. 45) intra- $d \rightarrow d^*$ transition between crystal-field split levels is out of our spectral range. No specific decrease of the interference pattern strength has been observed in this relatively thin $\text{Zn}_{1-x}\text{Fe}_x\text{Se}$ films either.

4. $\text{Zn}_{1-x}\text{Mn}_x\text{Se}$

In the $\text{Zn}_{1-x}\text{Mn}_x\text{Se}$ system we did not find evidence of charge-transfer transitions. In general, the Mn^{2+} system is expected to have a larger charge-transfer energy (i.e., a larger on-site Hund's rule exchange energy) in comparison with Co^{2+} or Fe^{2+} , because it has an exactly half-filled d^5 (6A_1) state, which is quite stable. Therefore, the

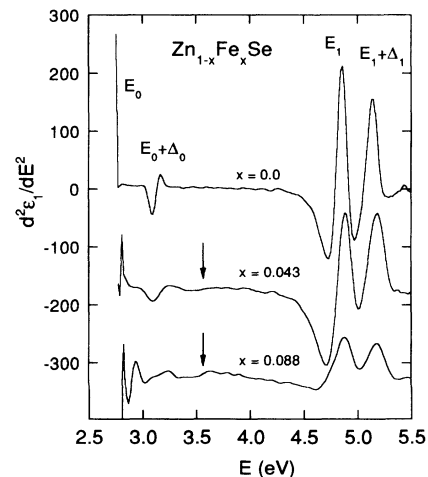


FIG. 8. Second derivative spectra of $\text{Zn}_{1-x}\text{Fe}_x\text{Se}$ alloys. In the $x = 0.043$ and 0.088 samples, a growing peak at around 3.6 eV is shown which cannot be misunderstood as the $E_0 + \Delta_0$ peak.

structure may be out of our spectral range, at greater than 5.5 eV, or the small effect of the charge-transfer transition to the dielectric function may be obscured by the huge structure associated with the E_1 and $E_1 + \Delta_1$ transitions. The intra- $d \rightarrow d^*$ transition between crystal-field split levels of Mn^{2+} in ZnSe has an approximate energy of 2.3 eV, and is observed in many optical measurements at low temperature.^{2,46} In our room-temperature study such a transition is not observed. Because of the thin-film thickness, the change of the interference pattern intensity could not be studied.

To confirm our interpretation of these features, systematic photoconductivity or phot capacitance studies of the $Zn_{1-x}(Mn,Fe,Co)_xSe$ systems are needed. Photoemission and inverse-photoemission experiments should also reveal precise charge-transfer transition energy values, and can help provide a better understanding of the electronic structure of these II-VI dilute magnetic semiconductor systems.

IV. CONCLUSIONS

We observed distortions in the interference patterns of $Zn_{1-x}Co_xSe$ at 1.6–1.8 eV which we interpreted as the

observation of intra- d -shell transitions of Co^{2+} in the tetrahedral crystal field of ZnSe. The $E_0 + \Delta_0$ structure was observed in $Zn_{1-x}Co_xSe$ up to $x = 0.04$. An additional peak at 4.3 eV is interpreted as a local Se $4p$ to Co $3d$ charge-transfer transition. The conduction gap at ~ 2.2 eV observed in the phot capacitance measurement was also manifest in our spectra as a systematic decrease in the interference patterns with Co concentration. We interpret this as a nonlocal charge-transfer transition. The roughly 2-eV energy difference between local and nonlocal charge-transfer processes can only be understood through a many-body approach. The same analysis has also been applied to explain an absorption peak at 3.6 eV in the $Zn_{1-x}Fe_xSe$ system. For the $Zn_{1-x}Mn_xSe$ system, no specific features associated with Mn $3d$ electrons have been observed in our room-temperature spectra up to 5.5 eV.

ACKNOWLEDGMENTS

This work was supported by NSF No. DMR89-20538 and DOE Grant No. DEFG02-91ER45439. The work at NRL was supported by the Office of Naval Research. Y. D. Kim is also supported in part by Research Institute for Basic Sciences, Kyung Hee University.

- ¹N. B. Brandt and V. V. Moshchkalov, *Adv. Phys.* **33**, 193 (1984).
- ²J. K. Furdyna and J. Kossut, in *Semiconductors and Semimetals*, edited by R. K. Willardson and A. C. Beer (Academic, San Diego, 1988), Vol. 25.
- ³W. A. Harrison, *Electronic Structure and the Properties of Solids* (Dover, New York, 1989).
- ⁴A. Zunger, *Electronic Structure of 3d Transition-Atom Impurities in Semiconductors*, Vol. 39 of *Solid State Physics*, edited by F. Seitz, D. Turnbull, and H. Ehrenreich (Academic, New York, 1986).
- ⁵A. Fazzio, M. J. Caldas, and A. Zunger, *Phys. Rev. B* **30**, 3430 (1984).
- ⁶J. Dreyhsig, H. E. Gumlich, and J. W. Allen, *Phys. Rev. B* **48**, 15 002 (1993).
- ⁷Y. D. Kim, S. L. Cooper, M. V. Klein, and B. T. Jonker, *Phys. Rev. B* **49**, 1732 (1994).
- ⁸Y. D. Kim, Y. C. Chang, and M. V. Klein, *Phys. Rev. B* **48**, 17 770 (1993).
- ⁹G. A. Sawatzky and J. W. Allen, *Phys. Rev. Lett.* **53**, 2339 (1984).
- ¹⁰J. Zaanen, C. Westra, and G. A. Sawatzky, *Phys. Rev. B* **33**, 8060 (1986).
- ¹¹G. v. d. Laan, C. Westra, C. Haas, and G. A. Sawatzky, *Phys. Rev. B* **23**, 4369 (1981).
- ¹²N. F. Mott, *Proc. R. Soc. London Ser. A* **62**, 416 (1949).
- ¹³N. F. Mott, *Philos. Mag.* **6**, 287 (1967).
- ¹⁴J. Hubbard, *Proc. R. Soc. London Ser. A* **227**, 237 (1964).
- ¹⁵J. Hubbard, *Proc. R. Soc. London Ser. A* **281**, 401 (1964).
- ¹⁶L. Ley, M. Taniguchi, J. Ghisen, and R. L. Johnson, *Phys. Rev. B* **35**, 2839 (1987).
- ¹⁷J. Zaanen, G. A. Sawatzky, and J. W. Allen, *Phys. Rev. Lett.* **55**, 418 (1985).
- ¹⁸A. J. Fujimori and F. Minami, *Phys. Rev. B* **30**, 957 (1984).
- ¹⁹D. E. Aspnes, *Opt. Commun.* **8**, 222 (1973).
- ²⁰D. E. Aspnes and A. A. Studna, *Appl. Opt.* **14**, 220 (1975).
- ²¹J. E. Potts, H. Cheng, S. Mohapatra, and T. L. Smith, *J. Appl. Phys.* **61**, 333 (1987).
- ²²K. Ohkawa, T. Mitsuyu, and O. Yamazaki, *Phys. Rev. B* **38**, 12 465 (1988).
- ²³W. Bala, M. Drozdowski, and M. Kozielski, *Phys. Status Solidi A* **130**, K195 (1992).
- ²⁴Y. D. Kim, S. L. Cooper, M. V. Klein, and B. T. Jonker, *Appl. Phys. Lett.* **62**, 2387 (1993).
- ²⁵D. E. Aspnes and A. A. Studna, *Phys. Rev. B* **27**, 985 (1983).
- ²⁶A. Savitzky and J. E. Gollay, *Anal. Chem.* **36**, 1627 (1974).
- ²⁷M. Cardona, *Modulation Spectroscopy*, Suppl. 11 of *Solid State Physics*, edited by F. Seitz, D. Turnbull, and H. Ehrenreich (Academic, New York, 1969).
- ²⁸D. E. Aspnes, in *Handbook on Semiconductors*, edited by M. Balkanski (North-Holland, Amsterdam, 1980), Vol. 2, p. 109.
- ²⁹P. Lautenschlager, M. Garriga, L. Viña, and M. Cardona, *Phys. Rev. B* **36**, 4821 (1987).
- ³⁰S. Adachi and T. Taguchi, *Phys. Rev. B* **43**, 9569 (1991).
- ³¹J. M. Baranowski, J. M. Allen, and G. L. Pearson, *Phys. Rev.* **160**, 627 (1967).
- ³²E. M. Wary and J. W. Allen, *J. Phys. C* **4**, 512 (1971).
- ³³J. M. Noras, H. R. Szawelska, and J. W. Allen, *J. Phys. C* **14**, 3255 (1981).
- ³⁴K. Klein, J. Dreyhsig, H.-E. Gumlich, M. Thiede, G. Goetz, H.-J. Schulz, and J. W. Allen, *Phys. Status Solidi A* **130**, K207 (1992).
- ³⁵R. M. A. Azzam and N. M. Bashara, *Ellipsometry and Polarized Light* (North-Holland, Amsterdam, 1977).
- ³⁶R. H. Good and T. J. Nelson, *Classical Theory of Electric and Magnetic Fields* (Academic, New York, 1971), p. 357.
- ³⁷B. T. Jonker, S. B. Qadri, J. J. Krebs, G. A. Prinz, and L. Salamanca-Young, *J. Vac. Sci. Technol. A* **7**, 1360 (1989).

- ³⁸B. T. Jonker, J. J. Krebs, G. A. Prinz, X. Liu, A. Petrou, and L. Salamanca-Young, in *Growth, Characterization and Properties of Ultrathin Magnetic Films and Multilayers*, edited by B. T. Jonker, J. P. Hermans, and E. G. Marinero, MRS Symposia Proceedings No. 151 (Materials Research Society, Pittsburgh, 1989), p. 151.
- ³⁹C. Chen, X. Wang, Z. Qin, W. Wu, and W. Girit, *Solid State Commun.* **87**, 717 (1993).
- ⁴⁰Y. D. Kim, M. V. Klein, S. F. Ren, Y. C. Chang, H. Luo, N. Samarth, and J. K. Furdyna, *Phys. Rev. B* **49**, 7262 (1994).
- ⁴¹D. S. McClure, *J. Chem. Phys.* **38**, 2289 (1963).
- ⁴²F. J. Morin, *Phys. Rev.* **93**, 1195 (1954).
- ⁴³D. S. McClure, *Electronic Spectra of Molecules and Ions in Crystals* (Academic, New York, 1959), p. 138.
- ⁴⁴H. H. Tippins, *Phys. Rev. B* **1**, 126 (1970).
- ⁴⁵K. P. O'Donnell, K. M. Lee, and G. D. Watkins, *J. Phys. C* **16**, L723 (1983).
- ⁴⁶Y. R. Lee, A. K. Ramdas, and R. L. Aggarwal, *Phys. Rev. B* **38**, 10 600 (1988).